Microfluidic laminate-based phantom for diffusion tensor-magnetic resonance imaging

2011 J. Micromech. Microeng. 21 095027

(http://iopscience.iop.org/0960-1317/21/9/095027)

J. Micromech. Microeng. **21** (2011) 095027 (11pp) doi:10.1088/0960-1317/21/9/095027

Microfluidic laminate-based phantom for diffusion tensor-magnetic resonance imaging

R Samuel[1,3], H J Sant[1], F Jiao[2], C R Johnson[2] and B K Gale[1]

[1] State of Utah Center of Excellence for Biomedical Microfluidics, University of Utah, 50 S Central Campus Dr., Rm 2110, Salt Lake City, UT 84112, USA
[2] Scientific Computing and Imaging Institute, University of Utah, 72 S Central Campus Dr. Rm 3750, Salt Lake City, UT 84112, USA

E-mail: raheel.samuel@utah.edu, himanshu.sant@utah.edu, bruce.gale@utah.edu, fjiao@sci.utah.edu and crj@sci.utah.edu

Received 15 April 2011, in final form 5 July 2011
Published 19 August 2011
Online at stacks.iop.org/JMM/21/095027

Abstract
This paper reports fabrication of a magnetic resonance imaging (MRI) phantom created by stacking of multiple thin polydimethylsiloxane (PDMS) layers. PDMS is spin-coated on SU-8 molds to obtain the desired layer thickness and imprints of the microchannel patterns that define the phantom geometry. This paper also identifies the unique challenges related to the fabrication and assembly of multiple thin layers and reports for the first time assembly of a large number of thin laminates of this nature. Use of photolithography techniques allows us to create a wide range of phantom geometries. The target dimensions of the phantoms reported here are two distinct stacks of 30 thin PDMS layers each of 10 μm thickness with either (i) curved 5 μm $\times$ 5 μm microchannels with 8.7 μm spacing, or (ii) straight 5 μm $\times$ 5 μm microchannels with 3.6 μm spacing. SEM scans of the assembled phantoms show open microchannels and a monolithic cross section with no visible interface between PDMS layers. Based on the results of diffusion tensor magnetic resonance imaging scanning, the anisotropic diffusion of water molecules due to the physical restriction of the microchannels was detected, which means that the phantom can be used to calibrate and optimize MRI instrumentation.

(Some figures in this article are in colour only in the electronic version)

1. Introduction

Molecular diffusion refers to the random movement of molecules through space, driven by their internal thermal energy. It is a process that is highly sensitive to the physical structure of the microscopic environment. Diffusion tensor magnetic resonance imaging (DT-MRI) has been used to measure the diffusivity of water and metabolites noninvasively at microscopic length scales [1, 2]. DT-MRI measures the restricted random Brownian motion of water molecules [3]. During the MRI measurement interval (ms), the water molecule can diffuse a distance of 5–20 μm, while the diffusion tensor at each voxel measures the local diffusion profile. For the standardization of DT-MRI machines, standard physical models (also known as phantoms) are required with well-defined microscopic architecture. A proposed design for an MRI phantom is shown in figure 1. Artificial fiber diffusion phantoms have been fabricated using hemp, linen, polyamide, polyester, polyethylene and rayon [1]. However, it is important to develop artificial phantoms that can be reproduced in order to produce a particular MRI scan result, which will help in efforts for the validation of MRI technology. The quality of a phantom is typically dependent on the anisotropy of water diffusion (restricted random Brownian motion of water molecules) and the amount of water in the phantom, which in turn determines the phantom design. The size of the PDMS-based phantom developed in this work was 1.5 cm $\times$ 1.5 cm $\times$ 0.3 mm to obtain an image of about 15 $\times$ 15 voxels of 0.5 mm or 1 mm cubes.

[3] Author to whom any correspondence should be addressed.

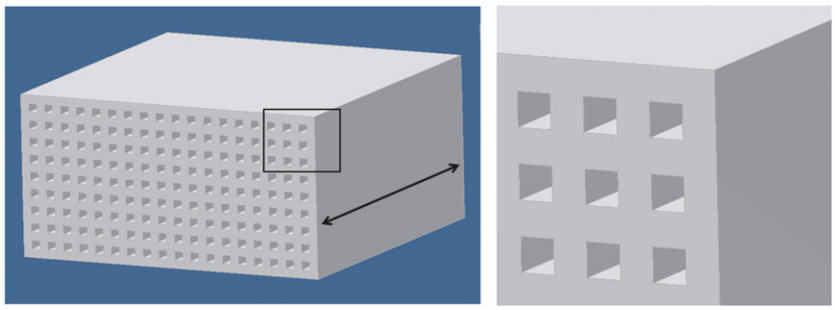

Figure 1. Left: a 3D schematic of the envisioned multilayer phantom (not to scale), the targeted dimensions are height: 0.3 mm, width: 1.5 cm, length: 1.5 cm. Each layer is 10 μm thick with 5 μm $\times$ 5 μm channels. Spacing between channels (3.6 or 8.7 μm) and the orientation (curved channels or straight channels) is varied for each phantom. The diffusional direction of water molecules is shown by the double-headed arrow. Right: a magnified view of the cross-sectional area marked by a black square in the left picture (small microchannels can be observed). With microfabrication techniques, we can reproduce such highly parallel, multilayered microchannels consistently.

PDMS is a popular material for biomedical applications because of its outstanding material properties and the simplicity with which it can be cast onto microstructured molds [4]. Most PDMS-based microfabricated products require micromolding of microchannels in PDMS layers and later bonding of these layers to glass/silicon or to another PDMS surface for the realization of the final product. Currently, soft lithography-based PDMS layer fabrication uses two approaches: spin-casting or the membrane-sandwich method [5, 6]. However, PDMS has its own microfabrication challenges. Peeling off a freely suspended spin-cast, $\sim$10 μm thick PDMS layer, from a molding substrate such as a silicon wafer is a significant challenge. Such thin layers are very delicate and once torn are easily damaged during the peeling process [7]. However, in some cases PDMS layers as thin as 70 nm and without embedded structures have been spun-cast and later peeled off. Demolding these layers requires the presence of an adhesion reduction layer between PDMS and the silicon substrate [8]. There are further hurdles in stacking these ultra-thin, spin-coated layers—the occurrence of air bubbles and wrinkles. However, researchers have been able to efficiently stack five relatively thick (120 μm) PDMS layers for 3D microfluidic channel realization by using the membrane-sandwich method [6], and a variation of the same method was used to assemble six (50 μm thick) layers [9]. In the membrane-sandwich method, uncured PDMS is placed between a SU-8 mold and a flat rigid plate. The flat rigid plate is pressurized from the top, which in turn squeezes the PDMS in between the mold and plate. Different layer thickness can be achieved by varying the applied pressure. After applying the required pressure, the whole assembly is heated and the PDMS layer cures, which is then peeled off the mold. The membrane-sandwich method [5, 6] allows great control in the fabrication process [10] but is limited to relatively thick and mechanically weaker layers (>20 μm) [11].

The geometry of the phantoms described in this paper was determined by the requirement of high MRI signal to noise ratio. During MRI scanning, high signal to noise ratios can be achieved if the phantoms can retain large amounts of water (i.e. a high ratio of combined microchannel volume/phantom volume) and high diffusion anisotropy. Consequently, each phantom layer necessitated a dense array of parallel microchannels and the layers needed to be as thin as could be handled easily and manufactured with high reproducibility. Based on these design criteria, the thickness of the PDMS layers was set to 10 μm. Fabricating a 10 μm thick layer with thousands of 5 μm $\times$ 5 μm (approximately) patterned parallel microchannels in an area of 1.5 mm $\times$ 1.5 mm is more feasible when they are spin-cast on SU-8 molds in standard photoresist spinners (available in almost all microfabrication labs) than with the previously mentioned membrane-sandwich methods (with reference to their relatively large microchannel dimensions, larger layer thickness and low microchannel density per layer) [6, 9]. Another variation of the membrane-sandwich approach used by Zhang *et al* [9] for thin PDMS layer stacking is the use of fluorosilanes for selective transfer of the PDMS microstructure from mold to final assembly with an intermediate transfer step [9]. Success of such an approach remains to be investigated when very thin PDMS layers (<20 μm) for a dense network of molded microchannels need to be assembled. In contrast, our approach utilizes spin-cast PDMS layers that are mechanically stronger than standard casting as the stretching of polymer chains in the radial direction on spinning at high spin speeds improves mechanical strength significantly [11]. This helps in proper release of the highly patterned layer from the mold, without any damage and permanent deformation of the layer. However, stacking a large number ($\sim$30) of thin (<20 μm) spin-cast patterned PDMS layers has so far not been demonstrated in the literature.

This work reports a unique fabrication process for fabricating patterned 10 μm thick PDMS layers cast from a standard SU-8 soft lithographic mold into a 30-layer laminate. Each layer includes thousands of microchannels that are filled with deionized (DI) water. The layers are created using conventional spin-casting techniques on a large mold area and later stacked and bonded by a repeatable and uniform stacking method. The unique feature of this method is the use of a thick transfer ring, made from PDMS as well to transport and assemble the thin PDMS layers while allowing the use of a unique air-pressure technique to bond stacked layers activated by a corona discharge. This special air-pressure technique helps in stacking the layers without any trapped air bubbles or wrinkles. When the 30 layers are stacked, they are immersed in DI water and then sealed in a PDMS block before being used

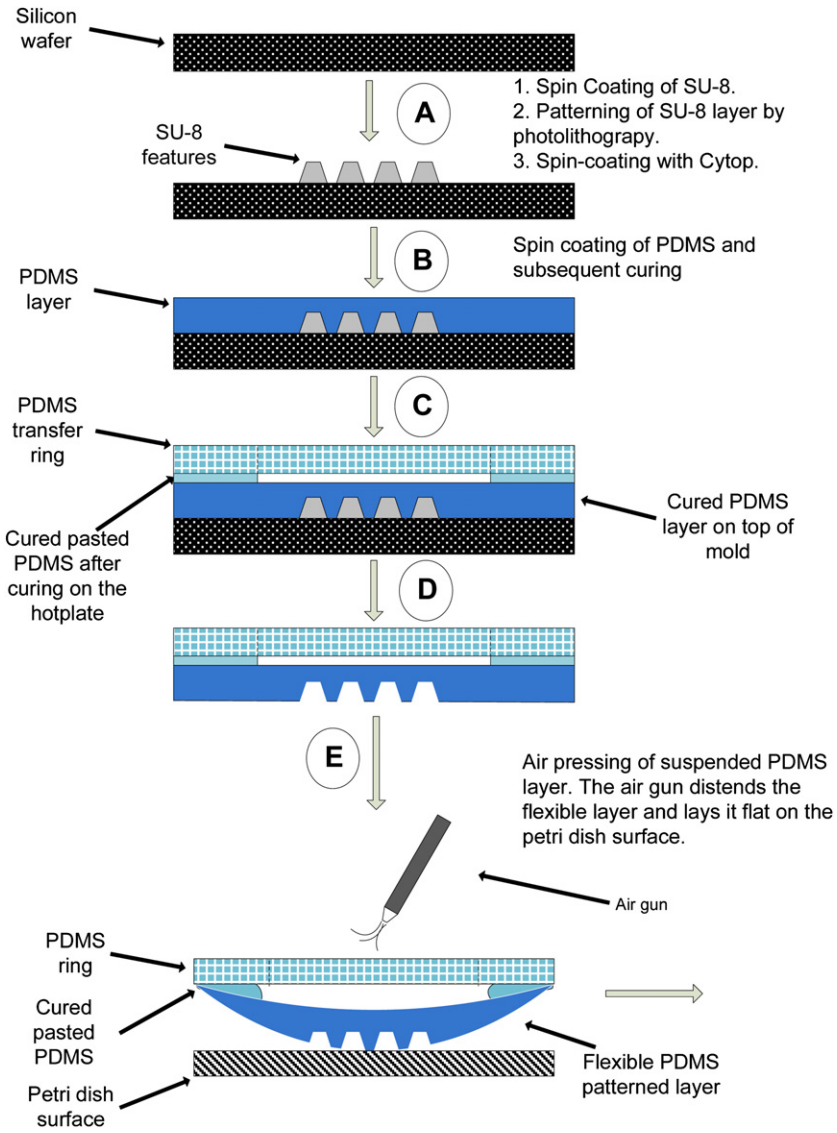

Figure 2. A schematic diagram of the phantom fabrication showing the PDMS softlithography steps, the use of the SU-8 mold and the transfer ring for the assembly of thin PDMS layers.

as a MRI phantom. By taking MR images of this phantom, researchers will be able to improve imaging characteristics of MRI machines.

2. Methods

The fabrication process used in this work is simple but can be best explained using three separate illustrations (figures 2–4), with the main steps designated in order and identified with a step number from A–M which is referred to in the description of the relevant process step.

2.1. SU-8 mold fabrication and pretreatment (step A, figure 2)

The individual patterned microfluidic laminates were created using SU-8 micromolding and PDMS soft lithography techniques in a normal room environment on a 4 inch silicon wafer (Silicon Qwest International Inc., Santa Clara, CA).

SU-8 2005 (Micro Chem, Newton, MA) was spun on the silicon wafer at 2500 rpm for 30 s at a ramp of 300 rpm s^{-1} and soft baked at 95 °C for 2 min on a leveled hot plate. The phantoms were fabricated using two mask patterns. One mask pattern generated a SU-8 mold with curved 5 μm wide channels with 8.7 μm channel spacing. The other mask pattern generated straight 5 μm wide channels with 3.6 μm channel spacing. An exposure bandpass filter (PL-360 LP, Omega Optical, Brattleboro, VT) was used to allow transmission of 365 nm wavelength light. A dose of 100 mJ cm^{-2} was used to expose ~5 μm thin SU-8 through the appropriate mask. The exposure time was set to 9 s on a mask aligner (EV-420, EV Group Inc. Tempe, AZ). After exposure, the substrate was post-baked for 3 min at 95 °C and later developed in the SU-8 developer for 2 min followed by isopropanol rinsing and drying with nitrogen gas. The patterned wafer was hard baked on a hotplate at 150 °C for 2 min.

Prior to micromolding the PDMS, the SU-8 mold was coated with a thin layer (~ 400 nm) of Cytop (CTL-809M,

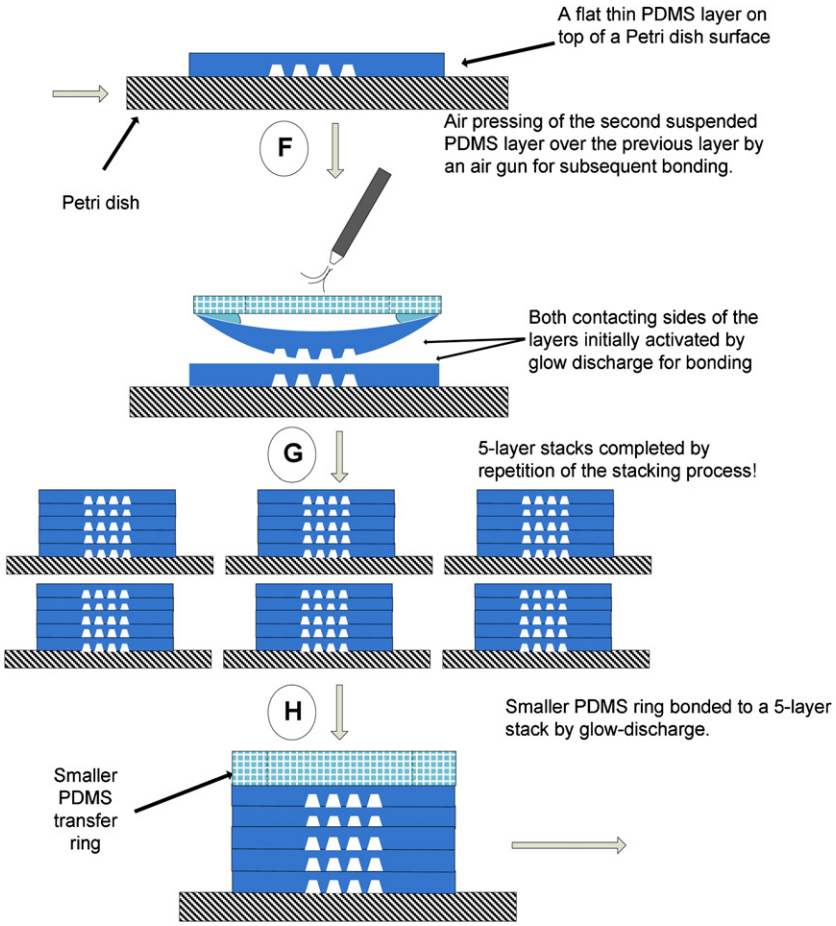

Figure 3. Summary of the fabrication process, depicting stacking of 30 layers to make six separate five-layer stacks. This approach improves the yield as any error during fabrication is limited to smaller stacks.

Asahi Glass Co. Ltd, Ibaraki, Japan). Cytop acts as an adhesion reduction layer between PDMS and silicon [8]. After the SU-8 hard bake, Cytop was spin-coated at 5000 rpm for 1 min with a 300 rpm s^{-1} ramp and cured at 180 °C on a leveled hotplate for 1 h.

2.2. PDMS molding (step B, figure 2)

Once the SU-8 mold was completed, the next step was to cast the PDMS layers on the mold. All the PDMS (Slygard® 184 Silicone Elastomer, Dow Corning, MI) used in this paper had the PDMS base to curing agent ratio of 5:1.

For layer fabrication, uncured PDMS was spun on the SU-8 mold with the overlying Cytop layer at 5000 rpm for 1 min (∼10 μm thick) (step B). The layer was cured at 100 °C for 10 min on a hot plate with an aluminum foil-cover to minimize foreign particulate contamination.

2.3. PDMS layer picking and assembly (steps C and D, figure 2)

At ∼10 μm, PDMS spin-cast layers have significant stress and are difficult to handle and tend to fold onto themselves. One of the challenges in this work was to remove such thin PDMS layers off the 4 inch SU-8 mold (large surface area) without damaging the very small molded microchannels on the layer or the layer itself or any of the microstructures across the substrate. To facilitate easy removal of the thin PDMS layer, a 3 mm thick transfer ring was made which had an outer diameter of 135 mm and inner diameter of 68 mm. The transfer ring was used as a holder that bonds the ends of the PDMS layer to lift the thin layer. Furthermore, the transfer ring provided a mechanical support to the thin layer after peeling it off from the mold. The ring was made using the standard PDMS casting process to make a PDMS slab and then a razor was used to core out the ring-shaped PDMS. In preparation for picking up the thin layers, uncured PDMS was applied using a spatula to the ends of the PDMS layer overlying the SU-8 mold. The uncured PDMS was applied such that it formed a ring on the overlying PDMS layer. This ring of uncured PDMS had an outer diameter the same as that of the mold (100 mm) and inner diameter of approximately 75 mm. In this way, the uncured PDMS did not interfere with the patterned microstructures (in the center of the layer) on the thin PDMS layer, overlying on the SU-8 mold. The transfer ring was placed on the mold such that it made a good contact with the uncured PDMS (step C). Both the mold and transfer ring on top of the PDMS were placed on a hotplate at 100 °C for 5 min. This process resulted in adhesion of the thin layer to the transfer ring. For PDMS layer removal, the transfer ring was first gently separated from

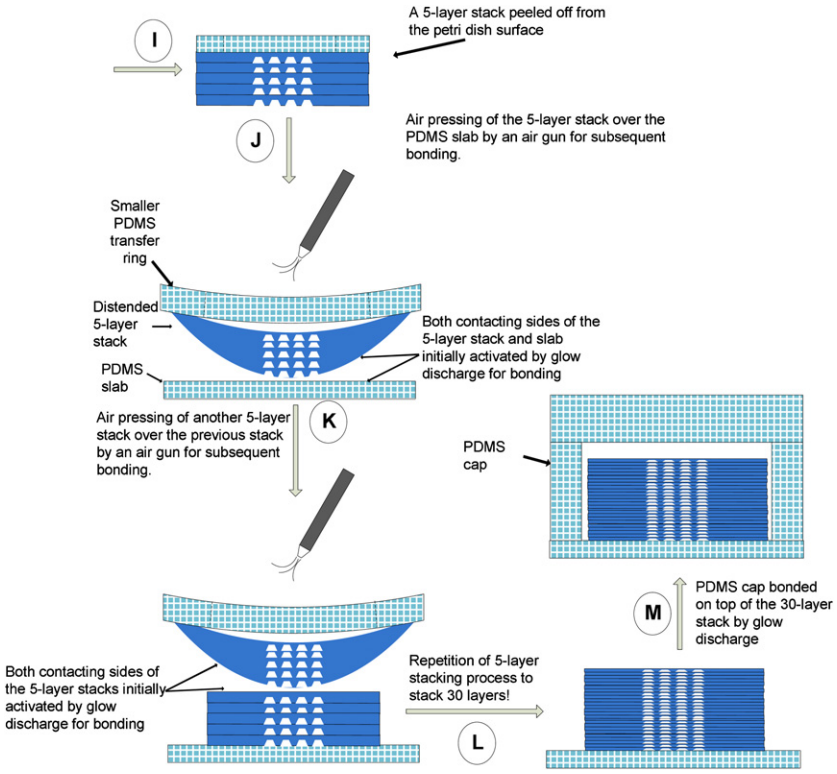

Figure 4. Summary of the fabrication process, depicting stacking of six five-layer stacks to make a single 30-layer stack and encasement of the stack by a PDMS cap for the realization of the final product.

the mold's edges. The transfer ring was then slowly pulled up from the mold from one end to the other, and the thin PDMS layer was brought with it, ensuring peeling off the thin PDMS layer without tearing (step D).

2.4. Stacking of the layers (step E, figure 2; steps F–H, figure 3; steps I–L, figure 4)

Each molded layer had up to 16 distinct phantom designs on it. A single microfluidic phantom was a 30 layer-laminate of only one of these 16 distinct designs (we used two of these designs to make two distinct microfluidic phantoms mentioned in this paper).

The main challenge of this work was the stacking of large number of highly flexible thin PDMS layers (at least 30 layers, to reach the minimum stack height for the MRI scanner used in this study), without the presence of any trapped air bubbles, wrinkles and delamination of the bonded layers. The stacking methodology had to be simple enough to be carried outside the clean room without the use of any complicated hardware, so as to be cost effective.

A Petri dish (Part 0875713, Fisher Scientific, Pittsburgh, PA) was used as the base while stacking the layers, as the polystyrene Petri dishes have low adhesion between Petri dish surface and cured PDMS, which provides an easy removal of the stacked PDMS laminates. After peeling off the PDMS layer from the mold, it was placed on a Petri dish gently by using air pressure to lay it flat (step E). Care was taken to make sure that no air bubbles formed between the PDMS layer and the Petri dish. Wrinkles and bubbles were avoided by bringing one end of the suspended layer in contact with the Petri dish surface and pressing it flat with air pressure (using a low-pressure compressed-air nozzle), starting from one end and progressively moving to the other end. The PDMS layer was separated from the transfer ring with a knife cut to release the transfer ring. There was enough room for the knife cut, so as to avoid any permanent damage to the molded structures located near the center of the wafer. For addition of the second layer, both mating surfaces were activated with a corona/glow discharge (LM4243-05, Enercon Industries Corporation, WI). The second layer was gently placed on top of the first layer using the same air-pressure technique and knife cut as described earlier (step F). No special hardware was used for layer alignment and was done by the naked eye using phantom borders as alignment marks. The same procedure was repeated to assemble six separate five-layer stacks (step G). The phantom design for this study required a stack of 30 thin layers of PDMS microstructures. For optimal phantom performance, each layer had to be flat without any wrinkles, trapped air bubbles or any layer detachment. For efficient layer stacking and consistent fabrication yield, six separate stacks of five layers each were fabricated and then stacked on each other to make a single 30-layer stack.

To facilitate the handling of five-layer stacks, a smaller PDMS transfer ring was used. Corona (glow discharge) treatment was done on top of one of the five-layer stacks to be used as a base stack on which other five-layer stacks would be stacked. One side of the smaller transfer ring was also activated by corona discharge and that face was placed on top of the base stack and pressed for 2 min before peeling off

the base stack from the Petri dish (steps H and I). The bottom surface of the base stack which was previously in contact with the Petri dish was activated with corona and placed on top of a cured and corona-treated PDMS substrate of 10 mm thickness (step J). The base stack was laid flat on the PDMS substrate using the same compressed air-pressure technique as was described earlier and cut free from the transfer ring with a sharp knife. The entire assembly procedure was repeated until a phantom prototype with 30 layers was created (steps K and L).

2.5. Device testing

To ensure that the microchannels had not collapsed and were filled with DI water, scanning electron microscope (SEM) scans of a phantom model's (five-layer stack) cross section after immersing it in a pool of polystyrene beads and DI water were collected. The purpose was to fill the microchannels with water, which will carry the polystyrene particles along with it. When the water is evaporated, the entrained polystyrene particles can be detected by imaging the cross section (approximately mid-way across the length of the channels) of the five-layer stack, which will confirm that the channels are being filled with DI water.

To accomplish the filling of the phantom with water, the phantom model was placed in a Petri dish. The Petri dish was filled with DI water containing 10% (by volume) polystyrene microspheres of 0.202 μm diameter (Part 07304, Polysciences Inc., PA). The Petri dish was placed in a vacuum chamber at moderate vacuum (–26 inHg) for 2 min, which degassed the microchannels and filled them with water. The stack was washed with DI water and dried in an oven at 62 °C for 2 h. Later, the stack was cut in the middle, across the channels by a fine blade. The newly exposed cross section was imaged by a SEM.

2.6. Device assembly (step M, figure 4)

The 30 layers laminated in the end of step L in figure 4 were pressed flat by a small roller to ensure that all the layers were evenly bonded and no layer delamination occurred. The microchannels of the phantom prototypes were opened by cutting the edges of the channels with a fine blade. The entire phantom was sealed using a PDMS cap that was corona-bonded to the PDMS substrate (step M). The PDMS cap also outlined a reservoir area around the phantom that contained DI water. A 2 mm thick PMMA (Polymethyl methacrylate) sheet (25 mm × 25 mm) was bonded with double-sided tape in a polystyrene Petri dish, to make a mold for the PDMS cap. The entire phantom assembly was cured overnight in an oven at 65 °C to improve the bond strength between different layers of phantom and ensure a leak-proof seal between the PDMS substrate and the cap. After cooling of the phantom prototype, DI water was injected through the PDMS cap using a syringe with a 27G needle until the reservoir containing the phantom was completely filled. The holes made by the syringe needle were sealed using a silicone elastomer (734 Flowable Sealant, Dow Corning, MI) to prevent any DI water leaking out of the reservoir. The submerged phantom was placed in a vacuum chamber at moderate vacuum (-26 inHg) for 2 min to degas the microchannels and to ensure that they were completely filled with water.

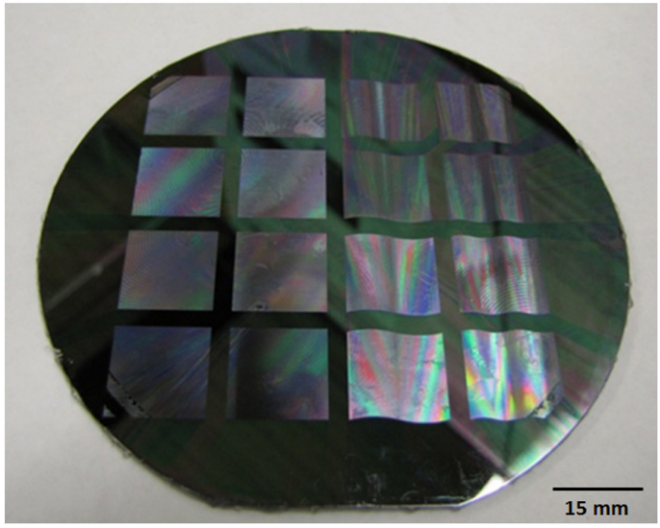

Figure 5. Photograph of the SU-8 mold with 16 distinct patterns, made using a 4 inch silicon wafer.

2.7. MRI imaging details

Imaging experiments of the MRI phantom were conducted on a Bruker Biospec 7 T horizontal-bore system (Bruker Inc, Billerica, MA) controlled by Paravision 5.0 software. For data acquisition, a standard 3D diffusion-weighted spin-echo sequence was used (in-plane resolution is 0.781 25 mm × 0.781 25 mm, and the slice thicknesses is 0.5 mm, diffusion-weighting b-value is 800 s mm^{-2}). For post-processing, diffusion tensors were computed on a voxel-by-voxel basis via weighted nonlinear least-squares fitting to extract the eigenvalues and their corresponding eigenvectors of the tensor matrix. The eigenvalues and eigenvectors correspond to the ensemble diffusivity and the ensemble diffusion directions of the local water molecules correspondingly.

3. Results and discussions

3.1. SU-8 mold fabrication

Figure 5 shows the SU-8 mold on a 4″ silicon wafer. This mold contained 16 distinct phantom designs on a 15 mm × 15 mm footprint. Exposure of the micropatterns was done such that the phantom of interest was placed at the center of the wafer. The patterns produced by the mold were found to be reproducible and meet the target width and spacing of the microstructures. Figure 6 shows an SEM scan of the cross section of the SU-8 mold used for phantom fabrication. The mold was diced in two by a wafer-dicing machine (DAD 641, DISCO Corp., Tokyo, Japan) and the newly exposed cross section was imaged by a SEM. The channel wall height of the mold was measured from the SEM scan and found to be 4.00 μm for an SU-8 2005 spun at a spin speed of 2500 rpm for 30 s, with ∼ 400 nm overlying Cytop layer.

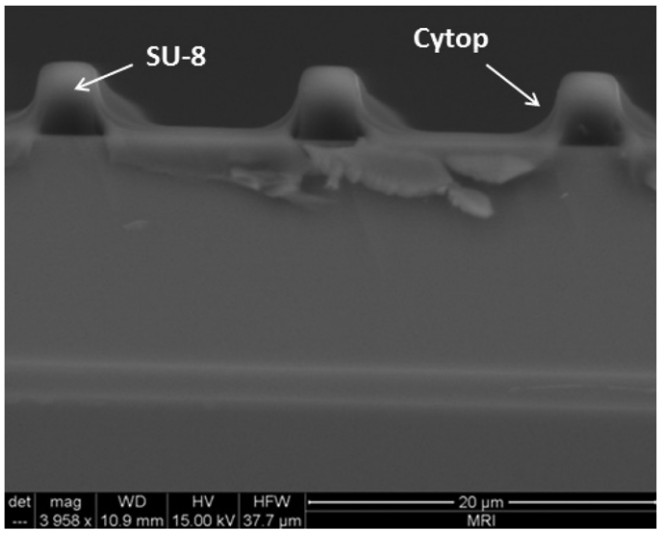

Figure 6. Picture showing SEM scan of the cross section of diced end of the SU-8 mold.

It should be noted that the same SU-8 mold was used to obtain all 30 layers for fabricating a microfluidic phantom. No damage or permanent deformation of the mold's microstructures was observed in the entire fabrication process of a single phantom.

3.2. PDMS molding: layer thickness and strength

In order to produce layers with precise thickness, the spinner was calibrated to achieve near-10 μm thick layers. Figure 7 shows a spin curve for PDMS spun on a 100-mm silicon wafer with a 400 nm overlying layer of Cytop. The thickness of each PDMS layer was measured by imaging the cross section of the layer under an optical microscope (Nikon Optiphot 88, Nikon Instruments Inc., Melville, NY). This method has been demonstrated to have reasonable accuracy (0.2%) for thin PDMS layer thickness measurements [12].

To determine the average thickness of each layer of the phantom, thicknesses of three individual five-layer stacks were measured at three distinct points. A total of nine data points were used to obtain an average individual layer thickness as 11.6 ± 0.5 μm.

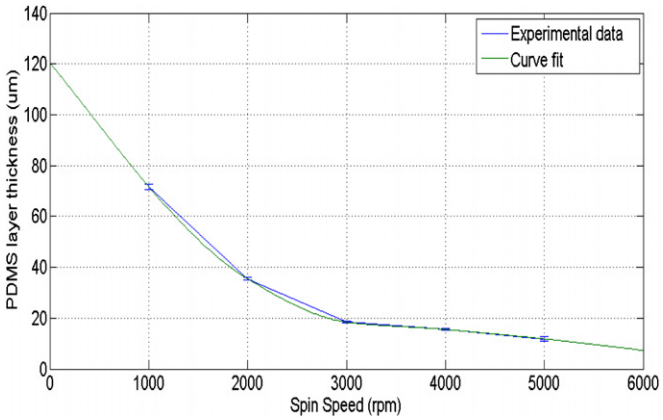

Figure 7. Plot of PDMS layer thickness (μm) versus spinner spin speed (RPM). The PDMS used for this work has the base to curing agent ratio of 5:1.

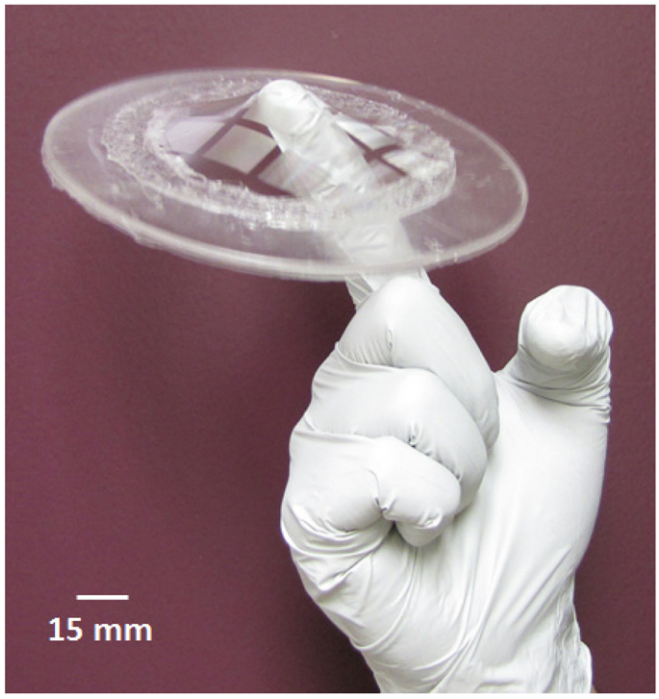

Figure 8. Picture of a PDMS transfer ring (weighing 30 g) being supported by ~10 μm thin membrane at the tip of a finger.

Interestingly, these thin PDMS membranes even with phantom microstructures proved to be very strong even at ~10 μm thickness. Figure 8 shows a picture of the PDMS layer attached to the transfer ring (weighing 30 g) being held at the center with the tip of a finger. This result is in accord with Liu *et al* [11] and very useful while picking up the layers and aligning them to fabricate a stack of multiple laminates.

3.3. PDMS layer picking and assembly

Figures 8 and 9 show the transfer ring that is used to pick up individual PDMS layers from the SU-8 mold. While some of the microstructures are lost because of the transfer ring overlay (figure 9), the single layer can be lifted off the mold cleanly without any effect to the layer structural integrity. In addition, this loss of microstructures due to the transfer ring overlay did not warrant any changes to the phantom design as the patterns in the center of the mold were of interest and used to fabricate all the phantoms we described in this paper. The *usable* phantom can be selected easily while aligning the mask to the SU-8 mold during exposure. However, the size of the uncured adhesive PDMS ring can be further optimized to provide the least overlay of the transfer ring onto the mold. Furthermore, a larger wafer can also be used to leave enough distance from the edge of the mold to achieve the same effect.

The PDMS ring was 3 mm thick. We found that a thicker PDMS ring would not be flexible enough to facilitate peeling off the thin layers, while a thinner ring would be too flexible to provide sufficient mechanical support to avoid folding of

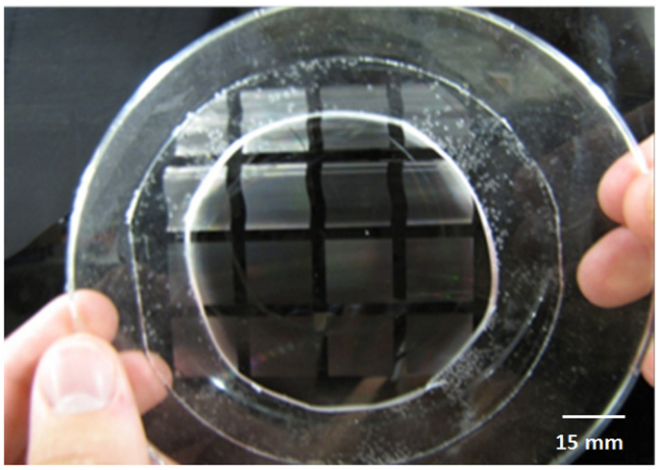

Figure 9. Picture of a PDMS transfer ring used to support and peel the thin layers of PDMS with microstructures. A supported PDMS layer with 16 distinct patterns (molded areas) can be seen in the picture.

the thin layer on itself. We were able to peel off at least 20 layers from a single PDMS ring before discarding it. After peeling off about 20 layers, the PDMS ring was not able to bond evenly to the thin layers and resulted in increased tearing of the thin layers during the peeling process. Bonding of the PDMS transfer ring to the thin PDMS layer on the SU-8 mold (shown in figure 5) was crucial for successful removal of the layer from the SU-8 mold. The bond had to be sufficiently strong and uniform at the ring and layer interface to overcome the stresses during peeling without tearing. We used two approaches to bond the PDMS ring to the PDMS layer overlying on the SU-8 mold: corona-discharge method and uncured PDMS as an adhesive. While the corona-discharge method was fast, it resulted in burnt PDMS particles on the thin layers (overlying the SU-8 mold) resulting in a damaged surface, which made the layer peeling very difficult. For this reason, a thin layer of uncured PDMS was used as an adhesive to bond the transfer ring to the thin layer on the SU-8 mold. Furthermore, different types of PDMS-to-PDMS bonding techniques have been evaluated for their bond strengths and using uncured PDMS as an adhesive for bonding has been shown to have the highest bond strength [13].

3.4. Stacking of the layers

The thin PDMS layers (containing microchannels) needed to be stacked with the least axial misalignment. The stacking in this case was done with the naked eye (with phantom borders as alignment marks) and may have some minor axial misalignments, but these misalignments can be reduced by stacking under a microscope or by utilizing an aligner specially designed to align PDMS layers [14]. The angular alignment of the microchannels along the length is very important for this application such that all the channels should point in the same direction to achieve high resolution and accuracy of the MRI scan. In future, a PDMS aligner may be used for more accurate alignment.

Figure 10 shows SEM (Quanta 600 FEG, FEI, OR) scans of the phantom model composed of a five-layer stack. The channels have a smooth trapezoidal cross section. The trapezoidal cross section is due to the overlying 400 nm Cytop layer, which was spin-coated after the SU-8 mold was made by photolithography. While the trapezoidal cross section of the channels does not affect the phantom performance, a thinner passivation layer can be obtained using fluoropolymers (monolayer thickness) that can be deposited by chemical vapor deposition [15], ion-sputtering deposition [16] or vacuum deposition [17] and subsequent evaporation if needed. The effect of using such a deposition approach on PDMS thin layer peeling remains to be investigated. Nevertheless, the large aspect ratio (channel length to height) and not the microchannel profile ensures anisotropic diffusion, the key requirement for MRI phantoms. Figure 11 shows the SEM scan of a 16-layer stack (consistent bonding between each individual layer should be noted). Figure 11 clearly shows no delamination for a stack of 16 layers, an important achievement for successful phantom fabrication.

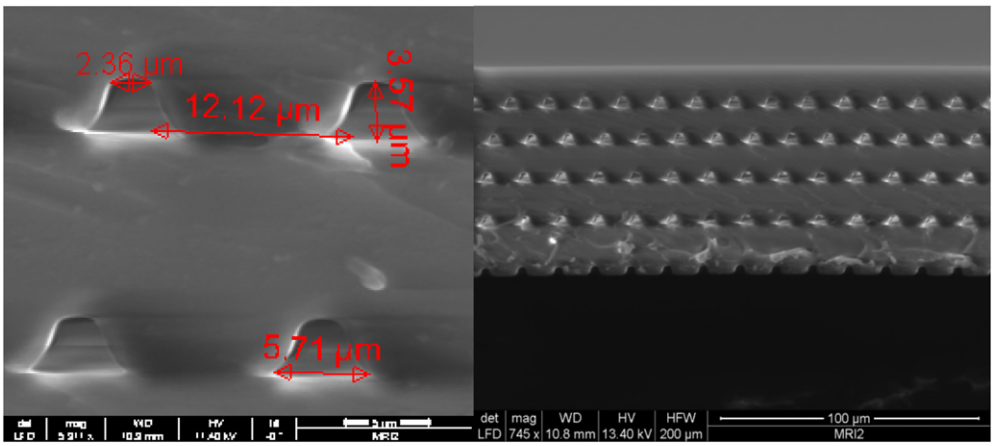

Figure 10. Image of a SEM scan of a five-layer stack of the PDMS layer showing the measured geometrical dimensions.

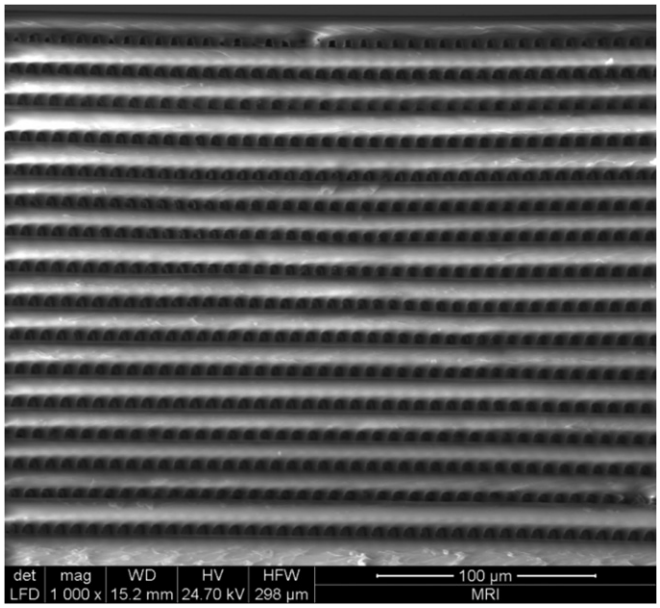

Figure 11. Image of a SEM scan of a 16-layer PDMS stack; the stack of layers after curing results in a monolithic structure with no visible interface separating the layers.

In figure 10, the height of the channels in the layers is 3.57 μm and about 0.43 μm smaller than the channel wall height (4.00 μm) in the mold. Possible reasons for this 0.43 μm difference are (i) shrinkage of PDMS on curing at a reasonably high temperature (100 °C) [18], (ii) relative stretching of the PDMS layer (during the bonding process) with respect to the previous bonded layer and (iii) variation in Cytop coating across the substrate. But such differences in channel parameters were allowable for this application. The layer channel height of 5 μm (if desired) can be obtained by varying the channel wall height in the mold to compensate for PDMS shrinkage and other effects. Furthermore, a Cytop layer of thickness less than 400 nm can be obtained by utilizing Cytop thinners available from Asahi Glass Co. Ltd, Japan.

3.5. Device testing

The newly exposed cross sections in the device testing (articulated in section 2.5) of the phantom were imaged by the SEM, and polystyrene particles were seen stuck on the inner microchannel walls in multiple scans (figure 12). This confirmed that the channels were being filled with DI

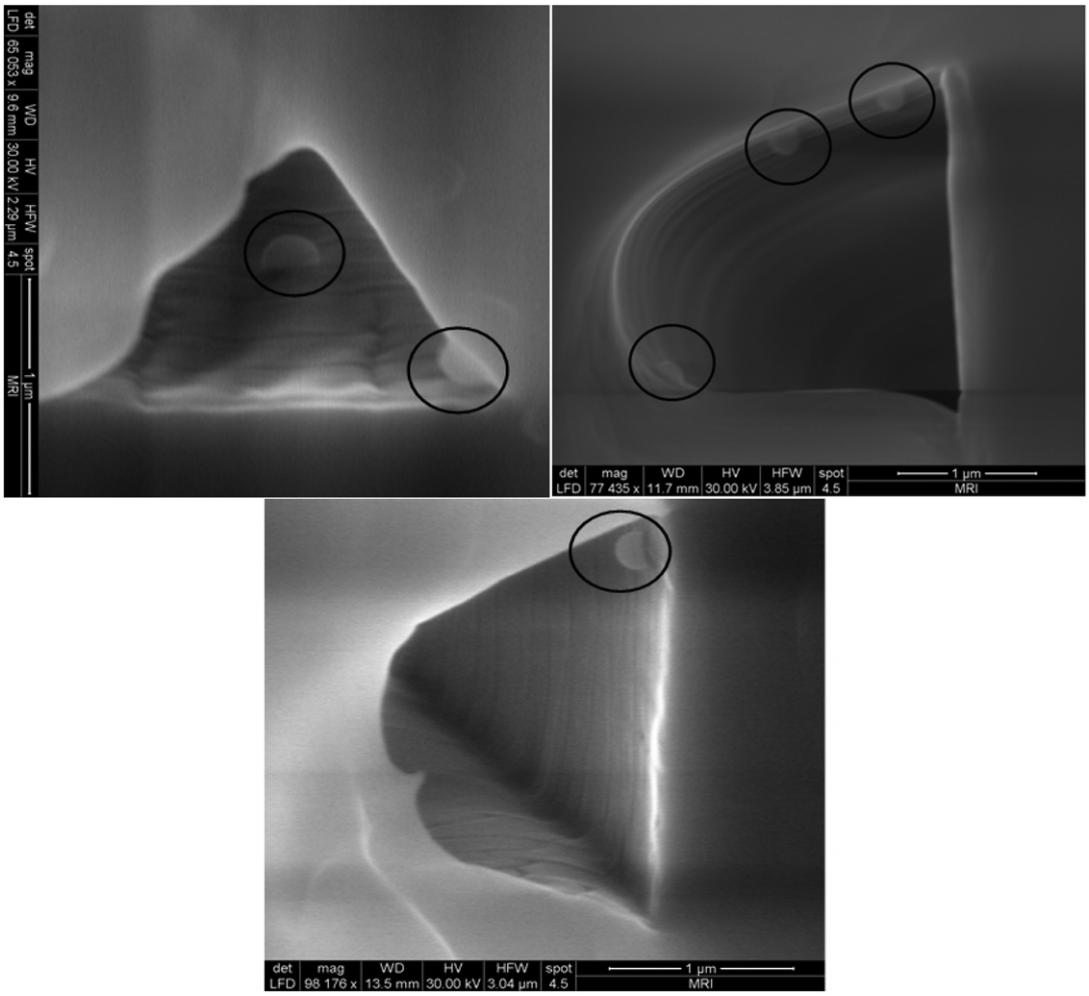

Figure 12. Images of SEM scans of microchannel cross sections showing polystyrene particles stuck on channel walls (particles marked by circles).

Figure 13. The pictures of two assembled MRI phantoms (left: with curved channels, right: with straight channels) along with a US quarter coin. Each phantom is placed in a square water reservoir formed by the PDMS cap and PDMS substrate. No air bubble can be seen in the phantom assembly.

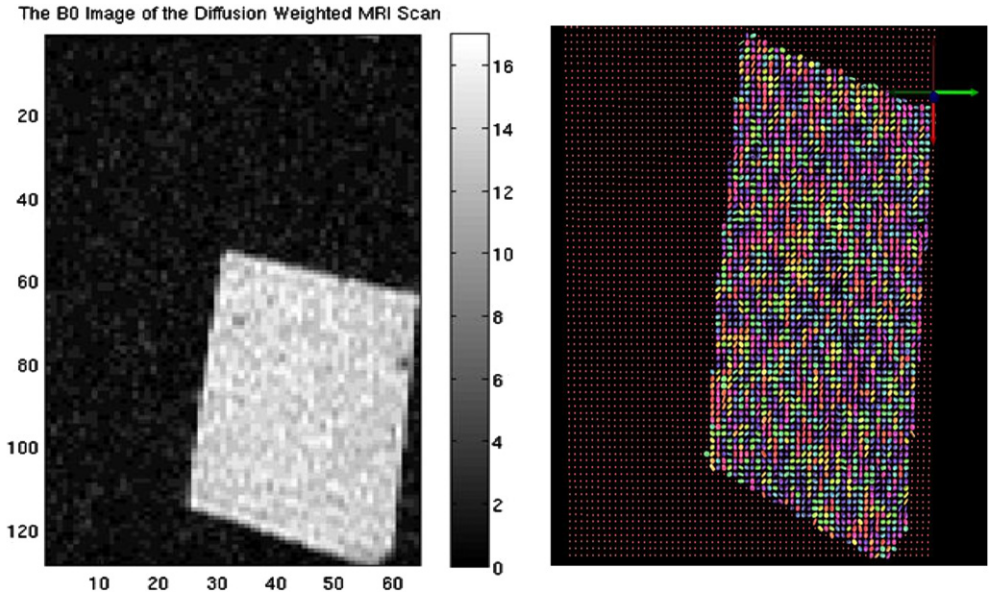

Figure 14. The B0 image (left-hand side) and the diffusion tensor image (right-hand side) of the phantom.

water and the polystyrene particles were carried inside the microchannels.

3.6. Device assembly

Figure 13 shows the fully fabricated MRI phantoms. The phantoms are immersed in a PDMS reservoir with DI water. The water infusion and air bubble withdrawal were done with 27 G non-coring needles attached to the plastic syringes.

3.7. Diffusion tensor imaging

Figure 14 shows the visualization of the B0 image (left) and the diffusion tensor image (right) of an MRI scan of the phantom shown in figure 13 (left). The diffusion tensor image's color variation depicts the alignment of the major eigenvector in different directions (x, y and z directions). From figure 14 (left), one can clearly see that the phantom was filled with water without any air bubbles (as the white area represents water and dark area represents absence of water). Based on figure 14 (right) the water molecule shows a certain degree of anisotropic diffusion. Due to the influence of the imaging background noise and possibly the misalignment between each stack, the anisotropy of each tensor is not as strong as expected. Additionally, the MRI instrumentation may not yet be able to adequately measure at these scales, so additional software development may be needed to better represent the movement of molecules in the phantom. Finally, the relative volume of water in the phantom may need to be increased to increase the signal available to the MRI instruments. Higher relative volumes of water would require higher aspect ratio channels with thicker layers, which is an ongoing effort.

4. Conclusion

A simple method of stacking patterned spin-coated $\sim$10 μm thick PDMS layers with densely packed microstructures has been developed and demonstrated. The stacking of up to

30 such layers has been performed without the presence of any trapped air bubbles or wrinkles. The unique layer-stacking technique can be used to fabricate MRI diffusion phantoms as gold standards for MRI machines. Furthermore, the methods developed in this project can be used to fabricate 3D structures in thin spin-coated PDMS layers, leading to sophisticated microfluidic chips fabricated with automated aligners for higher precision. The stacked layers were easy to handle once assembled and microchannels retained their cross section as evidenced by SEM scans. Additionally, the methods shown in this work allow for the assembly of large areas of thin layers with dense networks of microstructures with high repeatability and reproducibility. While the MRI phantoms reported here were fabricated in a normal laboratory environment, even better fabrication results in terms of layer bonding can be predicted if fabrication is carried out in a clean room environment.

Overall, we have presented a 30-layer MRI phantom fabricated with microfluidic laminates for the first time. A high signal to noise ratio during phantom scanning requires high water diffusion anisotropy and high water content inside the phantom channels, a significant challenge. Optimal dimensions and arrangements for the MRI phantom still need to be developed to improve the function of the phantom, though the methods presented here provide sufficient function to begin optimization of MRI algorithms for imaging of small fluid structures.

Acknowledgments

This work was funded in part by the NIH NCRR Center for Integrative Biomedical Computing (www.sci.utah.edu/cibc), NIH NCRR grant no 5P41RR012553-11 and NIH grant S10 RR023017 for supporting the Small Animal Imaging Facility. The authors thank Brian Baker and the nanofabrication facilities at the University of Utah for their help with this project.

References

[1] Fieremans E, Deene Y D, Delputte S, Ozdemir M S, Achten E and Lemahieu I 2008 The design of anisotropic diffusion phantoms for the validation of diffusion weighted magnetic resonance imaging *Phys. Med. Biol.* **53** 5405–19

[2] Tournier J-D, Yeh C, Calamante F, Cho K, Connelly A and Lin C 2008 Resolving crossing fibres using constrained spherical deconvolution: validation using diffusion-weighted imaging phantom data *NeuroImage* **42** 617–25

[3] Basser P J, Mattiello J and Lebihan D 1994 Estimation of the effective self-diffusion tensor from the NMR spin echo *J. Magn. Reson.* B **103** 247–54

[4] McDonald J C and Whitesides G M 2002 Poly(dimethylsiloxane) as a material for fabricating microfluidic devices *Acc. Chem. Res.* **35** 491–9

[5] Chiu D T, Jeon N L, Huang S, Kane R S, Wargo C J, Choi I S, Ingber D E and Whitesides G M 1999 Patterned deposition of cells and proteins onto surfaces by using three-dimensional microfluidic systems *Proc. Natl Acad. Sci. USA* **97** 2408–13

[6] Jo B, Van Lerberghe L M, Motsegood K M and Beebe D J 2000 Three-dimensional micro-channel fabrication in PDMS elastomer *J. Microelectromech. Syst.* **9** 76–81

[7] Sarma S and Krishnan S 2009 A process for manufacturing very thin PDMS films *Transactions of NAMRI/SME* **37** 277–83

[8] Thangawng A L, Ruoff R S, Swartz M A and Glucksberg M R 2007 An ultra-thin PDMS membrane as a bio/micro–nano interface: fabrication and characterization *Biomed. Microdevices* **9** 587–95

[9] Zhang M, Wu J, Wang L, Kang X and Wen W 2010 A simple method for fabricating multi-layer PDMS structures for 3D microfluidic chips *Lab Chip* **10** 1199–203

[10] Moraes C, Sun Y and Simmons C A 2009 Solving the shrinkage-induced PDMS alignment registration issue in multilayer soft lithography *J. Micromech. Microeng.* **19** 065015

[11] Liu M, Sun J, Sun Y, Bock C and Chen Q 2009 Thickness-dependent mechanical properties of polydimethylsiloxane membranes *J. Micromech. Microeng.* **19** 035028

[12] Zhang W Y, Ferguson G S and Tatic-Lucic S 2004 Elastomer supported cold-welding for room temperature wafer level bonding *IEEE Conf. MEMS 2004 Technical Digest (Maastricht, the Netherlands)* pp 741–4

[13] Eddings M A, Johnson M A and Gale B K 2008 Determining the optimal PDMS-PDMS bonding technique for microfluidic devices *J. Micromech. Microeng.* **18** 1–4

[14] Kim J Y, Baek J Y, Lee K A and Lee S H 2005 Automatic aligning and bonding system of PDMS layer for the fabrication of 3D microfluidic channels *Sensors Actuators* A **119** 593–8

[15] Lee K, Bhushan B and Hansford D 2005 Nanotribological characterization of fluoropolymer thin films for biomedical micro/nanoelectromechanical systems applications *J. Vac. Sci. Technol.* A **23** 804–10

[16] Quaranta F and Valentini A 1993 Ion-beam sputtering deposition of fluoropolymer thin films *Appl. Phys. Lett.* **63** 10–1

[17] Chen J, Ko F, Hsieh K, Chou C and Chang F 2004 Effect of fluoroalkyl substituents on the reactions of alkylchlorosilanes with mold surfaces for nanoimprint lithography *J. Vac. Sci. Technol.* B **22** 3233–41

[18] Lee S W and Lee S S 2008 Shrinkage ratio of PDMS and its alignment method for the wafer level process *Microsyst. Technol.* **14** 205–8